ISSN: 2581-8651
Vol-3, Issue-5, Sep – Oct 2021
https://dx.doi.org/10.22161/jhed.3.5.14
Peer-Reviewed Journal

Journal of Humanities and Education Development (JHED)

# The design and construction of a liquid damper for full-scale use in high-rise buildings

Seyednima Naghibi Iravani[1], Behnam Mehrkian[2]

[1]Islamic Azad University of Sofian
[2]RWTH Aachen University, Department of Civil Engineering, Mies-van-der-Rohe-Str. 1, Aachen 52074, Germany.
Corresponding Email: s.research68@yahoo.com

Received: 22 Aug 2021; Received in revised form: 20 Sep 2021; Accepted: 28 Sep 2021


***Abstract*****—** *To store surface water for various uses, the design of high dams and spillways has increased significantly. A review of the references indicates that in recent years, numerous studies have been conducted on the phenomenon of cavitation, ways to prevent its occurrence, and reducing the damages caused by this phenomenon on hydraulic and numerical models of free spillways. Numerical modeling of flow in pressurized tunnel spillways with aeration structures and studies related to the two-phase flow of water and air in these spillways are very few. Therefore, further understanding and recognition of the pressure fields and flow velocity near the aeration structure of pressurized tunnel spillways and the effect of the geometry of the aeration ramp and different aeration percentages on the flow require further studies. In this research, numerical simulation of the flow passing over the aeration ramp installed at the bottom of the pressurized duct has been studied. First, a numerical analysis of the hydraulic characteristics of the flow in the non-aerated state, such as the length of the rotation zone created downstream of the ramp, the intensity of turbulence, the pressure coefficients at the bottom of the duct, and the velocity and pressure profiles at different sections before and after the ramp, is carried out. Then, the effect of air entry in different percentages on various flow parameters, especially velocity profiles and pressure coefficients, is studied. The overall goal of this research is to correctly understand the hydraulic phenomena occurring in the two-phase flow of water and air near the tunnel overflow aerator.*

***Keywords*****— Tunnel spillway, cavitation, hydraulic characteristics, aeration, numerical simulation.**

## I. INTRODUCTION

For many years, incidents related to the phenomenon of cavitation have been attracting the attention of engineers in different parts of the world. The phenomenon of cavitation is a familiar phenomenon that is considered a major engineering hazard and challenge in most hydraulic structures that are exposed to high-speed flows, including dam overflows. Of course, it should be noted that the factor affecting this phenomenon is not limited to speed alone, and the existence of a set of multiple factors leads to the occurrence of this phenomenon. In tall spillways in the end areas, the flow velocity increases dramatically and the flow depth decreases. The combination of these factors reduces the cavitation index. As a result, a point in the structure with normal irregularity can become the starting point of cavitation in the structure.

In such a case, it is possible to prevent this phenomenon by reducing the flow velocity or increasing the flow pressure at the boundaries. It is important to note that the geometric shape of the spillway also plays a significant role in the occurrence or non-occurrence of cavitation. To prevent cavitation, the location of points where the pressure may decrease to the liquid vapor pressure with increasing velocity must be identified. Flow aeration, as an effective factor in eliminating or reducing cavitation-induced damage in free and tunnel spillways under pressure, has a significant impact on the hydraulic structure of the flow, including pressure and velocity fields.

In recent years, the correct understanding of the flow pattern and the effects of aeration in pressurized spillways with an aerated system has been among the topics studied by several researchers. Due to the specific complexity of two-phase flows and the lack of clarity on the exact relationship between flow aeration and reducing cavitation-induced damage, extensive studies are still needed on this issue. To store surface water for various uses, the design of high dams and spillways has increased

significantly. A review of the references indicates that in recent years, numerous studies have been conducted on the phenomenon of cavitation, ways to prevent its occurrence, and reducing the damages caused by this phenomenon on hydraulic and numerical models of free spillways (Aydin et al., 2020).

Numerical modeling of flow in pressurized tunnel spillways with aerated structures and studies related to the two-phase flow of water and air in these spillways is very limited. Therefore, further understanding and recognition of the pressure and flow velocity fields near the aerated structure of pressurized tunnel spillways and the effect of the geometry of the aerated ramp and different aeration percentages on the flow require further studies. In this study, numerical simulation of the flow passing over the aerated ramp installed at the bottom of the pressurized duct is addressed. First, a numerical analysis of the hydraulic characteristics of the flow in the absence of aeration is performed, such as the length of the rotation zone created downstream of the ramp, the intensity of turbulence, the pressure coefficients at the bottom of the duct, and the velocity and pressure profiles at different sections before and after the ramp.

Then, the effect of air inflow in different percentages on various flow parameters, especially velocity profiles and pressure coefficients, is studied. The overall goal of this research is to correctly understand the hydraulic phenomena occurring in the two-phase flow of water and air near the aerator of a tunnel spillway. Mankind has long been familiar with the construction of dams to meet its water needs. Since the last century, with the development of science and technology, the construction of various types of high dams by controlling surface flows has been developed to meet the needs of agricultural, industrial, drinking water, flood control, and hydroelectric power generation.

In these dams, the spillway, as one of the dependent hydraulic structures, plays a critical role in discharging the floods entering the dam reservoir with sufficient safety in a free flow or under pressure downstream. One of the major problems in high dam spillways is the possibility of cavitation and the resulting damage to the spillway bed and concrete walls, which not only disrupts the hydraulic performance of these structures and the dam but also causes significant damage to the spillway structure. Among the spillways that have been damaged by this phenomenon are the Glen Canyon Dam tunnel spillway in the United States and the Karun Dam free spillway in our country. In high dam spillways, due to the high flow velocity (more than 20 m/s), any change in the geometry of the channel, the roughness of the bed and wall, the curvature in the flow path, and the presence of operational joints in the wall cause the flow to separate from the channel wall and a local decrease in the pressure of the water vapor (Li et al., 2024, June).

In this case, when the cavitation phenomenon occurs, water at its ambient temperature changes from a liquid state to a vapor state, and cavitation bubbles (water vapor bubbles) are formed, which disappear as the water moves to areas of high pressure. The collapse of these cavitation bubbles is accompanied by the production of strong pressure waves caused by the explosion of the bubbles and the release of a significant amount of energy. If it occurs near the spillway wall, it causes erosion and corrosion of the concrete surface of the spillway and, if it continues, causes enormous damage to the wall and structure. Research conducted on the study of the cavitation phenomenon and methods for preventing it in spillways has shown that the use of resistant concrete and modifying the curvature and flow wall, stepped spillways, and aeration of the flow are suitable methods for preventing this phenomenon and reducing the damage caused by it.

Among them, the most effective and economical method for preventing and reducing the damages caused by this phenomenon is aeration. The entry of air into the flow in spillways causes changes in many flow characteristics, including changes in flow density, changes in velocity, and pressure, and changes in the turbulent state of the flow. Some of these changes are beneficial and others are harmful to the hydraulic system under study. The high cost and long duration of constructing hydraulic structures and the fact that testing is still the most accurate method for investigating the problems and issues facing such structures have prompted researchers and designers to seek to solve the aforementioned problems and issues by simulating real flow on physical models and conducting various tests.

For this reason, the use of numerical models has been greatly developed in recent decades. The most important advantage of a numerical computational estimate is its low cost and considerable speed. Also, numerical solutions to problems will give us complete information and the necessary details and will provide the values of the relevant variables throughout the study area. Contrary to the unfavorable conditions that arise during testing, inaccessible places in numerical computational work are few. No laboratory study can be expected to measure all the variables involved in the phenomenon under study in the entire flow field. Therefore, to complement the experimental data, a simultaneous numerical solution is also necessary.

## II. METHODOLOGY

In this study, the background of the research was familiarized by collecting and initially studying technical literature and research works related to flow aeration in high spillways, specially pressurized tunnel spillways. Then, by preparing a numerical model of the flow around the ramp-type tunnel spillway flow aerator installed in the pressurized flow bed, the flow was studied and analyzed. To prepare the numerical model used in this study, the Fluent 6.3.26 software was used. In the following, the governing equations of the flow and the methods for solving these equations in this software as well as the turbulence models used will be referred to.

The present study was conducted on a laboratory model of a water transfer tunnel (duct) with a square cross-section and an area of 100 cm2, which included an aerator ramp at the bottom of the duct, and aeration of the flow was carried out through pipes at the foot of the ramp. After validating the results and achieving the desired state, the scope of studies in the numerical model was increased and the effect of different aeration ramp geometries and different percentages of air entering the flow on the flow pattern, including velocity and pressure profiles, was studied.

In this chapter, the experimental model was first described, and then the different stages of preparing the numerical model, such as meshing and boundary and initial conditions, were examined, and the results of the numerical model, including its validation, were presented in the following chapters. Without a doubt, fluid dynamics software can be used when there is at least some knowledge of the governing equations for fluids. By introducing a general variable such as ϕ, the conservation or divergence form of all fluid flow equations, such as momentum and scalar values such as temperature and concentration of contaminants, can be written as follows:

$$\vec{V} = u\vec{i} + v\vec{j} + w\vec{k}$$

$$\frac{\partial(\rho\varphi)}{\partial t} + div\left(\rho\varphi\vec{V}\right) = div(\Gamma grad\varphi) + S_{\varphi}$$

Where is the velocity vector, $\rho$ is the fluid density, $\Gamma$ is the dispersion coefficient, is the quantity ϕ, and $S_{\varphi}$ is the spring term. The transport equation is a property of ϕ and clearly shows the different transport processes. The rates of change and transport are on the left side of the equation and the diffusion and source terms are on the right side of the equation. The Navier–Stokes equations are the conservation equations of flow, including the continuity, momentum, and energy equations. By substituting appropriate values into the equation, the continuity and momentum equations are obtained as the following relations:

$$\frac{\partial \rho}{\partial t} + \frac{\partial}{\partial x_i}(\rho u_i) = 0$$

$$\rho\left(\frac{\partial u_i}{\partial t} + u_j\frac{\partial u_i}{\partial x_j}\right) = B_i - \frac{\partial P}{\partial x_i} + \mu\left(\frac{\partial^2 u_i}{\partial x_j \partial x_j}\right)$$

In these equations, P is the dynamic pressure, and the other parameters are also specified. The equations generally express the continuity and momentum equations for incompressible flows, so to investigate the state of flow turbulence, it is necessary to derive the equations governing the flow in the turbulent state. Different flow regimes are determined based on the Reynolds number, which is the ratio of the magnitude of the inertial force to the viscous force. In experiments conducted on fluid systems, it has been observed that at a Reynolds number below a certain limit, called the critical Reynolds number, the laminar flow and adjacent layers slide over each other, which is called the laminar flow region (Iravani & Ahd, 2021). At Reynolds numbers higher than the critical number, serious changes are seen in the flow behavior, so that in this region of the flow, the velocity and other flow properties change completely irregularly and randomly. This region is called the turbulent flow region. Figure (1) shows the state of the flow layers near the wall and the point velocity of a turbulent flow.

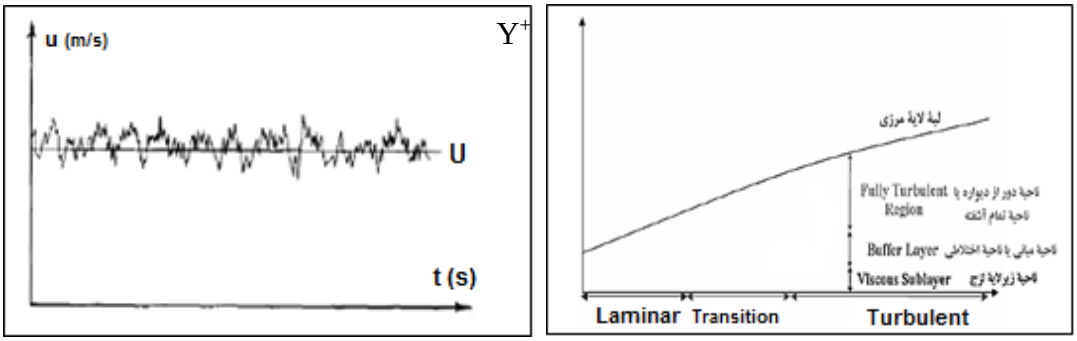


*Fig.1. Different layers of flow near the wall and the magnitude of the point velocity in turbulent flow*

The random nature of turbulent flows prevents the calculation and complete investigation of the motion of all fluid particles. Instead, the velocity can be divided into two parts: the constant average value U and the oscillatory component that is added to it. Therefore, considering the figure (1), the relationship below is obtained:

$$u = \overline{u_t} + u'_{(t)} = U + u'_{(t)}$$

Now, to obtain the governing equations in turbulent flows, the relation above must be applied to the relations provided to obtain the continuity and momentum equations in the turbulent flow state. The noteworthy point is that to apply the relation above to the aforementioned relations, the equations for the instantaneous quantities, i.e. the average quantities plus the oscillating quantities, are first written. Then, time averaging is performed on each side of the equation. After performing this operation, the continuity and momentum equations for incompressible turbulent flows are obtained from the relations below.

$$\frac{\partial u_i}{\partial x_i} = 0$$

$$\rho\left[\frac{\partial(\overline{u_i})}{\partial t} + (\overline{u_j})\frac{\partial(\overline{u_i})}{\partial x_j}\right] = B_i - \frac{\partial \bar{p}}{\partial x_i} + \frac{\partial}{\partial x_i}\left[\mu\frac{\partial \overline{u_i}}{\partial x_j} - \rho\overline{u_i' u_j'}\right]$$

The only difference between the momentum equation of turbulent flow and laminar flow is the addition of the last term on the right side of the equation, which is called turbulent stress or Reynolds stress. Equations together with the energy equation are called the RANS equations. These equations are explicit and no simplifying assumptions have been made in obtaining them, so these equations do not form a closed system, meaning the number of unknowns is greater than the number of equations. The results of the experiments conducted on the physical model available in the Department of Civil Engineering, UMIST University of Manchester have been used in this research.

The specifications of the laboratory model are shown in Figures. The tested section in the model included a horizontal duct with a square vertical cross-section of 100 cm2, which consisted of three different sections: transition, intermediate, and main sections. Upstream of the main section, a suitable length of duct has been considered for the development of the flow under laboratory conditions. A fixed-head water tank is located on the roof of the laboratory, which provides the flow rate for the experiments through a pipe with a diameter of 15 cm. The water flow passes through a contraction (converging) section with a wall angle of 7 ° and, over a short section, the flow is smoothed and enters the transfer section (He et al., 2024).

At the end of the main section, the flow diverges through a diverging section with a wall angle of 7 ° and is finally discharged into the water collection tank on the floor of the laboratory. All sections are connected by flanges with 8 bolts (Yip et al., 2021). The utmost care has been taken in installing the flanges and connecting the sections so that flow separation does not occur at the location of the flanges, which causes errors in the experiment the dimensions of the different sections of the duct are described.

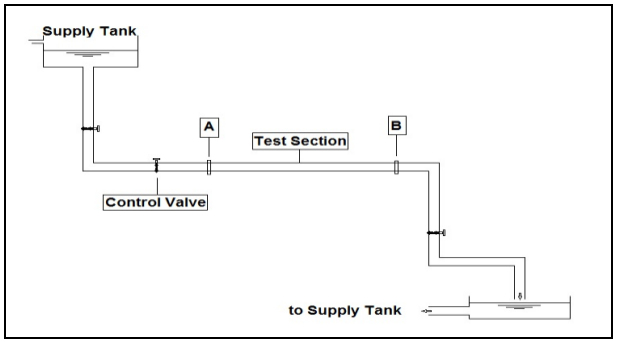


*Fig.2: Schematic diagram of the laboratory model*

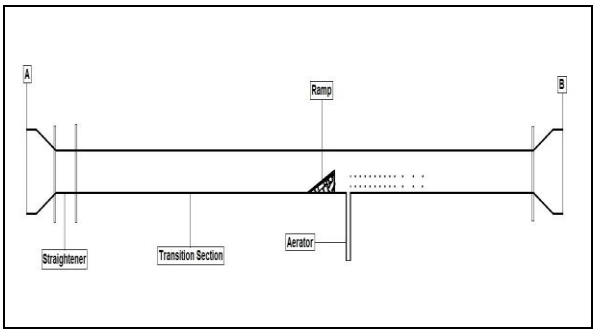


*Fig.3: Laboratory model test section*

*Table 1: Dimensions of different duct sections*

| Section | Cross-Sectional Dimension (m) | Length (m) |
|---|---|---|
| Contraction (A-B) | 0.15*0.15 – 0.1*0.1 | 0.2 |
| Straightener (B-C) | 0.1*0.1 | 0.145 |
| Transition Section (C-D) | 0.1*0.1 | 1.0 |
| Intermediate Section (D-E) | 0.1*0.1 | 0.3 |
| Main Section (E-F) | 0.1*0.1 | 0.9 |
| Diffuser (F-G) | 0.1*0.1 – 0.15*0.15 | 0.2 |

The flow rate in the duct is controlled by two valves, one upstream on the pipe connected to the water tank and the other downstream of the section under test. Also, the control valve located upstream of the main section is used

to stop the water flow in the duct when measuring devices such as transducers and air flow meters are adjusted or moved. Details of the ramps used in this study are given in Table (2). Where tr/d is the relative height of the ramp (ratio of the height of the ramp to the height of the duct).

*Table 2: Geometric details of the ramps used*

| Ramp | Height of Ramp (mm) | Length of Ramp (mm) | Angle of Ramp ($\theta^{\circ}$) | $t_r/d$ |
|---|---|---|---|---|
| A | 10 | 113.4 | 5 | 0.1 |
| B | 10 | 56.7 | 10 | 0.1 |
| C | 20 | 226.8 | 5 | 0.2 |
| D | 20 | 113.4 | 10 | 0.2 |

To investigate the pressure field in the cavity area, pressure transducers were placed in the duct floor through a series of holes created along the centerline of the duct floor downstream of the ramp. Pressure transducers were also installed in the walls. Therefore, the pressure values in the cavity area downstream of the ramp were accurately recorded (Lai et al., 2024). Also, at a section approximately 60 cm from the beginning of the ramp and upstream of it, which was considered a reference section, the pressure values were measured at the centerline of the duct floor and in the walls. The air inlet system into the flow consisted of 9 flexible plastic tubes with a diameter of 1 cm, which were installed in the duct floor a short distance from the foot of the ramp.

The air tubes were connected to the atmosphere (air pressure) on the other side. Along the air pipes, there were plastic valves that controlled the amount of air entering the flow, so the amount of air entering the flow during the experiment can be easily calculated in this way. Where the Reynolds numbers calculated are based on the height of the ramp. For the range of aeration ratios, the Weber number is in the range that, considering the range obtained, it can be concluded that surface tension does not have a significant effect on the results of the duct flow.

*Table 3: Experimental conditions and aeration ratios*

| Ramp | $t_r/d$ | Angle of Ramp ($\theta^{\circ}$) | Undisturbed Mean Velocity (m/s) | Reynolds Number ($Re*10^4$) | Aeration Ratio (%β) |
|---|---|---|---|---|---|
| A | 0.1 | 5 | 4.1 | 3.1 | 0, 2, 4, 6, 8 |
| B | 0.1 | 10 | 4.1 | 3.1 | 0, 2, 4, 6, 8 |
| C | 0.2 | 5 | 4.1 | 6.2 | 0, 2, 4, 6, 8 |
| D | 0.2 | 10 | 4.1 | 6.2 | 0, 2, 4, 6, 8 |

## III. FINDINGS

Many process flows are mixtures of phases. The physical phases of matter include gas, liquid, and solid. However, the concept of phase is used in a broader sense in multiphase flow systems (Tarpø et al, 2021). In multiphase flow, a phase is a separable part of the flow that responds to the potential field in which it is placed and interacts with other phases. For example, solid particles of different sizes of the same material can be considered as different phases because each set of particles of the same size will have a similar dynamic response to the flow field. Multiphase flow regimes can be divided into four general categories: gas-liquid or liquid-liquid, gas-solid, liquid-solid, and three-phase flows.

The development of computational fluid dynamics has provided the basis for a greater understanding of the dynamics of multiphase flows. Currently, there are two approaches to numerically calculating multiphase flows, Euler-Lagrange and Euler-Euler. In the Euler-Lagrange approach, first, the continuous phase of the flow is solved using the Euler equations, i.e. the Navier-Stokes equations, and then the second phase, for example, sediment particles, is examined from the Lagrangian perspective. But in the Euler-Euler approach, the second phase is also considered as a continuous phase, and, depending on the method used, either one equation is solved for all phases or a separate equation of the conservation equations is solved for each phase.

In the Euler-Euler approach, there are three types of methods, namely: VOF, Mixture, and Eulerian. The VOF method is a technique for tracing the interface of phases for a fixed Eulerian mesh. This model is designed for two or more immiscible fluids, whose interface location is of interest. In this method, a set of momentum equations is

assigned to the multiphase flow and the volume fraction of each phase in each computational cell is determined. The Mixture method is designed for two or more phases in which the phases are considered as a continuous interpenetrating medium the momentum equations for the mixed flow are solved and relative velocities are used to describe the dispersed phases The Eulerian method is the most complex multiphase method in Fluent software.

This method solves the momentum and continuity equations for each phase. These equations are related through the pressure and interphase exchange coefficients, which depend on the type of phases. The Mixture method is a simplified multiphase method that can be used to model multiphase flows where the phases move at different speeds. In this method, it is assumed that the phases have local equilibrium on a short spatial length scale, which allows the influence of the phases on each other to be considered. The Mixture method can model n phases by solving momentum, continuity, and energy equations for the mixed phase, volume fraction equations for the secondary phases, and algebraic relations for relative velocities. The relative velocity, which is the slip velocity, is defined as the velocity of the secondary phase (p) relative to the primary phase (q).

$$\overrightarrow{v_{pq}} = \overrightarrow{v_p} - \overrightarrow{v_q}$$

The mass fraction of each phase (k) is defined as the equation below, which is obtained using it and according to the drift velocity equation.

$$C_k = \frac{\alpha_k \rho_k}{\rho_m}$$

$$\overrightarrow{v_{dr,p}} = \overrightarrow{v_{pq}} - \sum_{k=1}^{n} C_k \overrightarrow{v_{qk}}$$

Using the continuity equation and drift velocity, the volume fraction equation of the secondary phase p is defined according to the equation below:

$$\frac{\partial}{\partial t}(\alpha_p \rho_p) + \nabla.(\alpha_p \rho_p \overrightarrow{v_m}) = -\nabla.(\alpha_p \rho_p \overrightarrow{v_{dr,p}}) + \sum_{q=1}^{n}(\dot{m}_{qp} - \dot{m}_{pq})$$

Where and are the mass transfer from phase q to p and the mass transfer from phase p to q, respectively? The volume fraction equation for the lesser phase is solved and the volume fraction of the remaining phase is calculated according to the constraint of the relation below.

$$\sum_{q=1}^{n} \alpha_q = 1$$

***Geometry and meshing of the numerical model.*** Gambit software was used to prepare the two-dimensional and three-dimensional geometry of the numerical model. In addition, Gambit can generate meshes and networks in computational fluid dynamics specifically. This software is a preprocessor for computational fluid dynamics software such as Fluent, whose outputs are used as input files for Fluent. In general, the steps of this preprocessor are as follows:

• Geometry generation: In this stage, geometry can be generated in this software, or geometry can be generated from other geometry-generating software such as AutoCAD and SolidWorks and introduced to this software.

• Mesh generation on geometry.

• Determination of boundary conditions and different areas.

Gambit software has many unique features in the field of meshing and meshing. In two-dimensional models, tetrahedral, trihedral, or a mixture of both meshes can be used. In three-dimensional mode, hexagonal, tetrahedral, pyramidal, or a mixture of these elements can be used.

***The meshing of the two-dimensional model.*** In this research, to conduct studies on the numerical model, first, the two-dimensional mode of the numerical model meshing was completely investigated, and then the three-dimensional mode was modeled, and the results obtained in two-dimensional and three-dimensional models were compared with each other. In the two-dimensional model, m 2 of the duct length was modeled, according to Figure (4). This length includes the main section some of its downstream and the transfer section. Also, m 0.05 of the length of the air transfer pipes downstream of the ramp was modeled.

To accurately examine the flow boundary layer and changes in flow parameters near the wall, a finer meshing was used in the walls, so that in different meshing cases, 3 to 7 cells near the walls became finer. In the case without aeration (single-phase flow), various turbulence models, including all k-ε and k- ε models, were used to model flow turbulence, and the results of these models were compared with each other. In the case of aeration (two-phase flow), the Mixture method was used to model the interaction between phases, and the RNG k-ε and SST k- ε turbulence models were used to model flow turbulence.

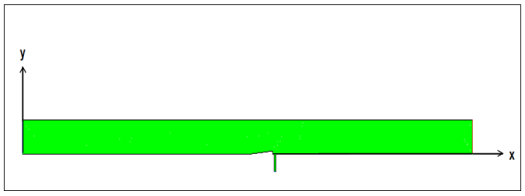


*Fig.4: Two-dimensional network of the flow field in the general case for ramp A*

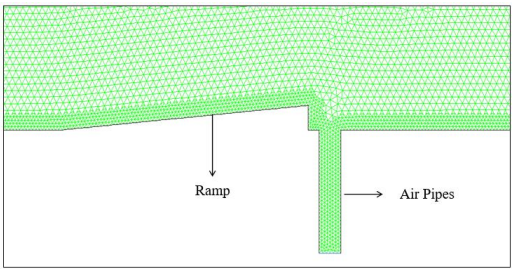


*Fig.5: Two-dimensional meshing of the flow field near ramp A*

***Sensitivity Analysis.*** The sensitivity of numerical models to model geometry, meshing, boundary conditions, and initial conditions has always been an important issue in numerical modeling. Mesh generation is considered one of the most important parts of the numerical solution, which is very effective in numerical solution accuracy. In this context, different patterns in the field of meshing have been presented in different numerical models, each of which has its strengths and weaknesses. In Fluent software, to make the results of numerical modeling as close as possible to the hydraulic model, the trial-and-error method should be used.

So by using different meshing in the numerical model and comparing the output results from the software with the results of the laboratory model, the most appropriate geometry and meshing were selected. In this research, computational cells with sizes of 0.002 m to 0.007 m were used. The sensitivity analysis of the numerical model was performed concerning the mesh size and it was found that in the two-dimensional and three-dimensional modes, using a grid with smaller cell dimensions than the grid created with computational cell sizes of 0.003 m and 0.004 m does not have much effect on the accuracy of the calculations.

Sensitivity analysis was also performed to determine the number of cells near the wall in the two-dimensional and three-dimensional models and it was found that to better match the results of the numerical model with the experimental results, 12 cells near the wall should be reduced. Also, in the numerical model, different sizes were considered for the length of the duct upstream of the ramp, and by performing the sensitivity analysis, it was found that a length of 1 m for the duct upstream of the ramp is sufficient for the complete development of the flow before reaching the ramp location.

## IV. CONCLUSION

The way the velocity changes in the direction of the flow and the average velocity vectors, especially in the rotation area, are important parameters expressing the state of the flow passing over the ramp. Figures (4-14) and (4-15) show the velocity meters in the direction of the flow and the average velocity vectors for the flow passing over the aeration ramp, for ramps B and D, respectively.

According to these figures, the velocity in the direction of the flow at the end of the ramp reaches its maximum value due to the presence of the ramp and the reduction in the cross-sectional area of the duct, and after entering the rotation area, it takes on negative values near the bottom of the duct, and gradually the negative values of the velocity decrease in the direction of the flow, and finally, at the end of the rotation area, the negative velocity is not observed, and then the flow returns to its normal state. According to the velocity meters, it is observed that the increase in flow velocity on the smaller angle ramps has a relatively uniform trend due to the gradual contraction of the duct cross-section, while on the larger angle ramps, this increase has occurred with greater intensity, and conversely, the decrease in flow velocity downstream of the larger angle ramps has occurred with less intensity. Also, the turning area immediately downstream of the ramp is visible in all cases.

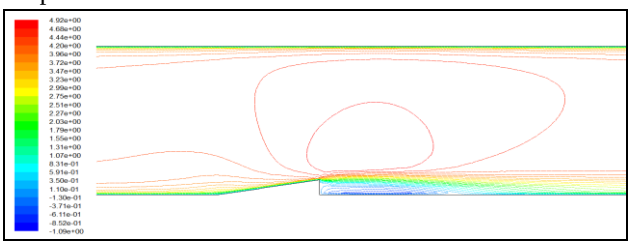

*Fig.6: Velocity meters in the flow direction*

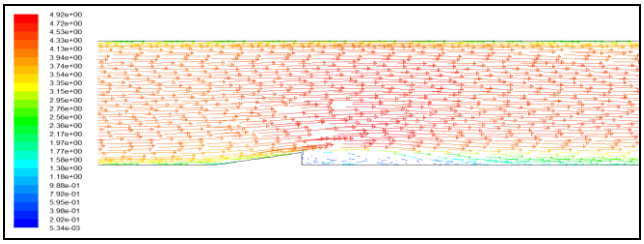

*Fig.7: Average flow velocity vectors*

**Pressure profiles.** Figure (8) shows the changes in CP ref obtained from the numerical model and the experimental results for different aeration percentages for ramp A and the correlation between the numerical and experimental results. The value of CP ref increases with increasing the percentage of air entering the flow. Due to the closed flow (the duct is under pressure), any change in the pressure values due to aeration near the ramp affects the entire flow, including the upstream. Therefore, with an increase in the percentage of air entering the flow, which leads to an increase in pressure in the cavity area, the pressure at the reference point also increases. The correlation coefficient between the CP ref obtained from the numerical model and the experimental results is 0.9422,

which indicates an acceptable simulation of the flow upstream of the ramp by the numerical model.

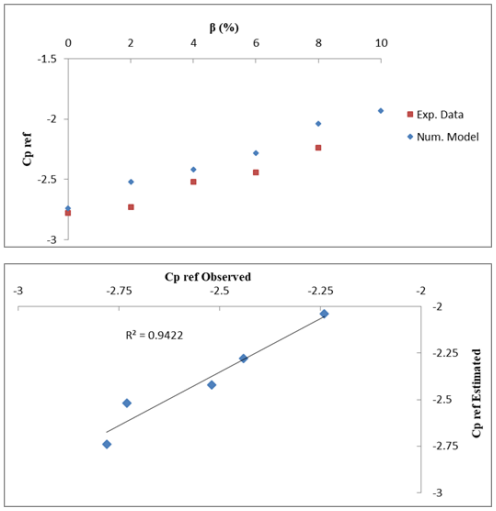


*Fig.8 - CP ref changes for different aeration percentages for ramp A and correlation of numerical and experimental results*

To show the effect of aeration at the ramp location on the duct pressure field, in Figure (8) the pressure profiles in the vertical sections of the duct flow for β=0%, %2 towards ramp D are displayed.

***No aeration condition***. In the case of water flow passing over the aerated ramp installed in the duct floor in the no aeration condition, the comparison of the results obtained from two-dimensional and three-dimensional modeling indicates a very small difference between them. The reconnection length (La) was estimated in two-dimensional modeling with a slight decrease compared to the laboratory results and in three-dimensional modeling with a slight increase. However, in the calculations of pressure coefficients and velocity profiles, no significant difference was observed between the two-dimensional and three-dimensional models.

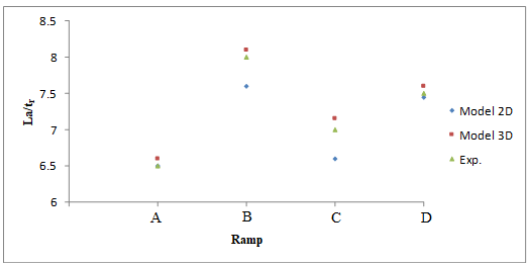


*Fig.9: Comparison of 2D and 3D model results for reconnection length for different ramps in the non-aeration state*

The complexities related to the multiphase nature of the flow, such as the interaction between phases, do not exist in the case of no aeration, and therefore the two-dimensional model estimates the flow characteristics such as the reconnection length and pressure coefficients as well as the three-dimensional model.

***Case with aeration.*** In this study, with the introduction of air into the flow, the equations related to multiphase flows dominate the problem, and therefore, modeling in the two-dimensional mode for estimating the cavity length (Lc) suffers from a greater error than in the three-dimensional mode. In both the two-dimensional and three-dimensional modes, the cavity length downstream of the ramp was estimated to be less than the experimental results. The interaction between the phases and the small geometric dimensions of the duct and ramp are among the reasons for the error in modeling the two-phase flow of water and air passing over the ramp embedded in the bottom of the duct in the two-dimensional mode. However, there is no significant difference between the two-dimensional and three-dimensional models in calculating the pressure coefficients and velocity profiles.

## REFERENCES

[1] Aydin, A. C., Yaman, Z., Ağcakoca, E., Kiliç, M., Maali, M., & Aghazadeh Dizaji, A. (2020). CFRP effect on the buckling behavior of dented cylindrical shells. International Journal of Steel Structures, 20, 425-435.

[2] Iravani, S. N. N., & Ahd, P. D. R. S. (2021). Examining Strain and Bending Deformation Parameters From Nonlinear Static Analysis of Concrete, Reinforced Concrete, and Fiber-Reinforced (FRP) Concrete Samples. Turkish Journal of Computer and Mathematics Education (TURCOMAT), 12(1), 7719-7728.

[3] Tarpø, M., Georgakis, C., Brandt, A., & Brincker, R. (2021). Experimental determination of structural damping of a full-scale building with and without tuned liquid dampers. Structural Control and Health Monitoring, 28(3), e2676.

[4] Yip, C. C., Wong, J. Y., Ling, L., Goh, Y. L., & Ong, H. E. (2021). Dynamic response of scaled structure with one liquid tuned mass damper. Case Studies in Construction Materials, 14, e00512.